Progr Colloid Polym Sci (2006) 133: 52–57
DOI 10.1007/2882_062

Published online: 28 April 2006

Dzina Kleshchanok
John E. Wong
Regine v. Klitzing
Peter R. Lang

Potential Profiles Between Polyelectrolyte Multilayers and Spherical Colloids Measured with TIRM

Dzina Kleshchanok · Peter R. Lang (✉)
Forschungszentrum Jülich, IFF, Weiche Materie, 52425 Jülich, Germany
e-mail: p.lang@fz-juelich.de

John E. Wong
RWTH Aachen, Institut für Physikalische Chemie, Landoltweg 2, 52056 Aachen, Germany

Regine v. Klitzing
Christian-Albrechts-Universität, Institut für Physikalische Chemie, Ludewig-Meyn-Str. 8, 24118 Kiel, Germany

Abstract We investigated the potential profile between colloidal probes floating above a polyelectrolyte multilayer (PEM), built up by the layer by layer technique with Total Internal Reflection Microscopy (TIRM). The interaction between a single poly(ethyleneimine) layer and an amino-terminated polystyrene latex sphere can be accurately described by the superposition of electrostatic repulsion and gravity. PEM with more than one layer exhibit laterally inhomogeneous potentials with extremely long ranging repulsive contributions.

Keywords
Polyelectrolyte multilayers · Total internal reflection microsocopy · Interaction potential

Introduction

Polyelectrolyte Multilayers

The ongoing miniaturization of devices causes a further increasing interest in ultrathin coatings of interfaces, because such films serve to modify surface properties in an easy and controlled way. In the early 1990s Decher and coworkers proposed a new technique to prepare ultra-thin polymer films. Polyelectrolyte multilayers (PEM) can be prepared with the layer-by-layer (LbL) method [1, 2] by alternating adsorption of polyanions and polycations from aqueous solutions. The main feature of PEM is, that the film thickness can be easily tuned to Ångstrom precision by the number of deposited layers or the ionic strength of the ployelectrolyte solution. Further, the macroscopic properties (optical or conductive) are controlled by the type of polyelectrolyte used for the preparation. Besides planar surfaces also colloidal particles can be coated [3] or even objects with a highly irregular shape.

During the adsorption process of a new layer, polyanion/polycation complexes are formed with the formerly adsorbed polyelectrolyte layer [4] due to the exchange of the counterion by the oppositely charged polyelectrolyte. This means that most of the charges within the polyelectrolyte multilayer are compensated by the opposite polymer charges and not by small counterions. A consequence of this "intrinsic" charge compensation might be the strong interdigitation between adjacent layers found by neutron reflectometry [5–7]. The rms-roughness of the internal interfaces can be of the order of the thickness of a single layer.

One of the questions still under discussion concerns the driving force for the multilayer formation. For a long time, electrostatic attraction between polylelectrolytes in solution and the oppositely charged surface was discussed as the only driving force for the formation of multilayers [2]. Indeed, it has been shown that a minimum polymer charge density is required for the formation of multilayers [8–11]. Electrokinetic measurements at multilayer coated colloidal particles in an electrical field show that the potential changes sign after each adsorption step, i.e. the zeta-potential as a function of the number of adsorbed layers shows a kind of zig-zag curve with alternating charge sign (e.g. [3]). It is assumed that a charge reversal is required for the built-up of PEM.

On the other hand, this assumption is contradicted by the observation that PEM can be formed at an ionic strength of the polyelectrolyte solution as high as 1 mol/L. Since at these salt concentrations the electrostatic interactions are mostly screened (the Debye length is about 3 Å [11]), the PEM formation has to be driven by other effects. Another contradiction to the simple model of electrostatic attraction of polyelectrolytes by the surface is the fact that it is possible under certain conditions to build up consecutive layers of the same charge sign [12].

With regard to these observations the question arises what kind of surface potential is presented by the top layer to its surroundings. Since polyelectrolyte tails are directed towards the solution, it is assumed that electrokinetic experiments measure the potential at a kind of shear plane near the end of the tails. Of course the conformation of the tails can be changed due to the directional flux along the particles. The potential includes also all free and entrapped ions between the shear plane and the particle surface. All these factors could affect the surface potential and make it different from the local potential which the polyelectrolyte chains really experience. The same problems occur in streaming potential measurements, where a liquid flows along the surface [13]. The surface potential was also studied by static measurements like in a surface force apparatus (SFA) [12] or by an atomic force microscope (AFM) [14]. The SFA measures forces between two half cylinders normalized to their curvature raduis (typically 1–2 cm). This results in a very low lateral resolution. This problem is overcome in Colloidal Probe AFM studies where the AFM cantilever tip is replaced by a micron sized sphere, which determines the lateral resolution. In the present paper we propose a different technique, i.e. Total Internal Reflection Microscopy (TIRM) [15] to measure the surface potential. While TIRM and AFM provide roughly the same spatial resolution, the "force resolution" of TIRM is in the order of 0.01 pN, which is about two orders of magnitude higher than that of AFM.

Total Internal Reflection Microscopy

A charged colloidal sphere in solution, which sediments due to gravity will eventually come close enough to the bottom wall of the container, and experience electrostatic repulsion from that, if the wall carries like charges. The superposition of gravity and electrostatic leads to an interaction potential between the particle and the wall with a shallow minimum at a distance $h_{\min}$. However, the particle will not stay statically at this equillibrium distance. Due to Brownian motion it will rather sample a distribution of heights, $p(h)$, which is related to the interaction potential profile by Boltzman's equation

$$p(h) = A \exp\left\{-\frac{\phi(h)}{k_{\mathrm{B}}T}\right\} . \tag{1}$$

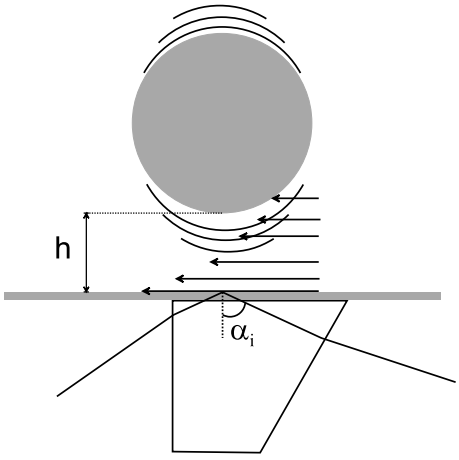

Fig. 1 Sketch of the evanescent wave optics

Here $p(h)\mathrm{d}h$ is the probability to find the particle in the height interval $h + \mathrm{d}h$ and A is a constant normalizing the integrated distribution to unity.

The height fluctuations resulting from the thermal motion can be directly observed by TIRM. For this purpose a Laser beam is directed via a prism to the container/solution interface as sketched in Fig. 1, with an incident angle α_i such that it is totally reflected. The electric field of the Laser beam penetrates the interface causing an evanescent wave, the amplitude of which decays exponentially with the distance from the interface. A single colloidal sphere, interacting with this evanescent wave will scatter light depending on its position as [16]

$$I_S(h) = I(h = 0) \exp\{-\xi h\} , \tag{2}$$

where h is the minimum distance of the sphere from the wall in the normal direction and ξ is the inverse penetration depth of the evanescent wave. By virtue of this relation the particle's height fluctuations will cause fluctuations of the scattered intensity and

$$p(I_S(h))\mathrm{d}I_S(h) = p(h)\mathrm{d}h , \tag{3}$$

where $p(I_S(h))\mathrm{d}I_S(h)$ is the probability to observe scattered intensity in the interval $I_S(h) + \mathrm{d}I_S(h)$. Introducing Eqs. 1 and 2 into Eq. 3 relates the the probability density of the scattered intensity to the interaction potential by

$$-p(I_S(h))\frac{I_S(h=0)}{\xi}\exp\{-\xi h\} = A \exp\left\{-\frac{\phi(h)}{k_{\mathrm{B}}T}\right\} . \tag{4}$$

In a typical TIRM experiment static scattering intensities are measured with a time resolution in the range of 10 ms, which translates as 3×10^4 data points recorded for a five minutes measurement. This is sufficient to make the normalized intensity histogram $N(I_S(h))$ converge to $p(I_S(h))$. Therefore, dividing Eq. 4 by the corresponding expression for the intensity which occurs with the highest

frequency, $I_S(h_m)$ yields

$$\frac{N(I_S(h))}{N(I_S(h_m))}\frac{I_S(h)}{I_S(h_m)} = \exp\left\{-\frac{\phi(h)-\phi(h_m)}{k_BT}\right\}. \quad (5)$$

When solving Eq. 5 for the potential difference $\Delta\phi = \phi(h)-\phi(h_m)$, it can be expressed as a function of four measurable quantities

$$\frac{\Delta\phi}{k_BT} = \ln\left(\frac{N(I_S(h_m))}{N(I_S(h))}\right) + \ln\left(\frac{I_S(h_m)}{I_S(h)}\right). \quad (6)$$

Finally, the second logarithmic term on the right hand side of Eq. 6 can be related to the particle's distance to the wall using Eq. 2

$$\frac{\Delta\phi}{k_BT} = \ln\left(\frac{N(I_S(h_m))}{N(I_S(h))}\right) + \Delta h\xi, \quad (7)$$

where $\Delta h = h - h_m$ and $\xi = 2\pi/\lambda_0\sqrt{(n_1\sin\alpha_i)^2 - n_2^2}$ with λ_0 the laser vacuum wavelength, n_1 and n_2 the index of refraction of the glass and the solvent, respectively. According to Eq. 7 it is possible to detect the potential *profile* in front of the surface by TIRM.

Experimental

Multilayer Preparation

Branched polyethylene imine (PEI) and poly(styrene sulfonate) sodium salt (PSS) were obtained from Aldrich (Steinheim, Germany). The molecular weight of PEI is 750 000 g/mol and 70 000 in the case of PSS. Poly(diallylamine dimethylammonium bromide) (PDADMAC) was a donation from Werner Jaeger (Fraunhofer Institute for Applied Polymer Research, Potsdam, Germany) and has a molecular weight of 100 000. The polymer solutions contained 10^{-2} monomol/l (concentration of monomer units) of the respective polyelectrolyte in Milli-Q-water. The dipping solutions were prepared in 0.1 molar NaCl without adjustment of pH. The substrates were conventional microscope slides and cleaned for 30 min in 1 : 1 H_20_2/H_2SO_4 mixture. After that they were coated with a PEI layer. On some substrates then, PSS and PDADMAC were deposited consecutively via the layer-by-layer technique by immersion for 20 min into the respective aqueous polymer solutions and by rinsing with Milli-Q-water three times after each deposition step. The films were dried in an air stream only after completion of the desired multilayer assembly.

TIRM

Our TIRM instrumentation is a home-built set-up, which was in parts assembled with standard microscope components from Olympus. We use a 15 mW HeNe-Laser with $\lambda_0 = 632.8$ nm to generate the evanescent wave. The Laser is mounted on a vertically oriented goniometer, to allow for the variation of incident angles, i.e. the variation of penetration depth. For all experiments of this contribution we applied an angle of incidence of 67.5 degree, which corresponds to a penetration depth of ca. 120 nm. Scattered light was collected through an infinity corrected objective (Olympus SLCPLFL 40X) and split into two paths both of which contained a tube lens to image the field of view either to the chip of a CCD-camera (JAI M1) or the photo-cathode of a photomultiplier tube (PMT) (Hamamatsu H7421-40). In the path of the PMT we introduced a diaphragm with a diameter of 400 μm in the image plane of the tube lens to cut off most of the observed background. This ensured a signal to noise ratio better than 25. The CCD-camera was used to make sure a single particle was located in the center of the area observed through the diaphragm. Since we did not apply optical tweezers and the particles are in thermal motion they have a limited residence time in the area observed through the diaphragm of the order of 10 minutes for a freely floating sphere of radius $R \approx 5$ μm. This limited the observation time to the range of about 300 seconds. The PMT was operated in the single photon counting mode with a time resolution of 500 ns. It was read out by a National Instruments counter card at a frequency of typically 100 to 1000 Hz. An example of the resulting intensity trace is shown in Fig. 2. For further evaluation the raw data were converted to intensity histograms and potential profiles using Origin (by OriginLab Corporation) work sheet scripts.

Two kinds of probe spheres were applied to measure the potential of differently charged top layers of the PEM-assembly. If the top layer was positively charged (PEI or PDADMAC) we used an amino-terminated polystyrene latex (Fisher Scientific) with a radius of $R = 2.92$ μm according to the manufacturer's specifications. To probe the negatively charged surface of PSS layers we used a polystyrene latex with sulfonate end-groups and a radius of $R = 4.54$ μm. In the following we will refer to these probes as PSA and PSS respectively. The latex spheres were diluted from their stock suspension down to a volume fraction of 10^{-8} and the solutions were contained in a carbonized PTFE-frame sandwiched between the PEM-coated microscope slide and a bare glass slide on top. The ionic strength of the solutions was adjusted by addition of NaCl if PSS top layers were to be probed and in the other cases HCl was added to adjust pH and ionic strength.

Results and Discussion

Raw data from a PSA-sphere floating above a glass slide coated with a single PEI-layer are shown in Fig. 2. The pH of the solution containing the PSA-particle was adjusted to 4 which corresponds to a Debye screening length of $\kappa^{-1} = 30$ nm. To check reproducibility we collected data from three different spheres. The resulting intensity

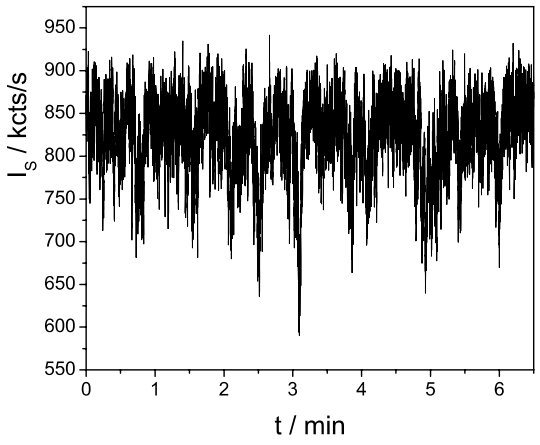

Fig. 2 Raw data of intensity vs time from a TIRM experiment on a 2.92 μm PSA sphere floating above a glass surface coated with a single PEI-layer

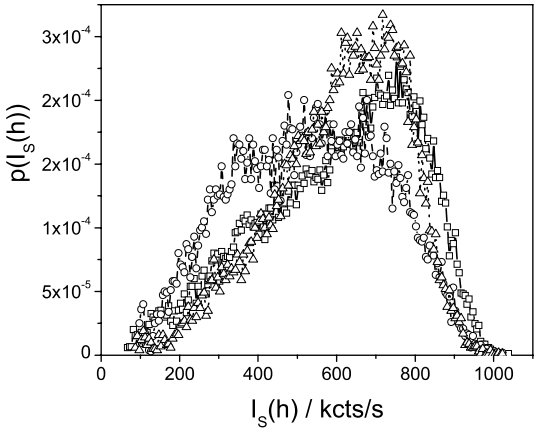

Fig. 3 Intensity histograms from TIRM experiments on PSA spheres floating above a glass surface coated with a single PEI-layer. Different line types and symbols represent different spheres at different locations

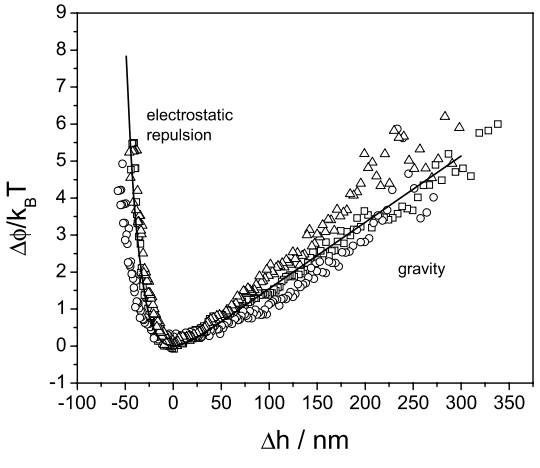

Fig. 4 Interaction potential between PSA spheres and a glass surface coated with a single PEI-layer. The potentials were calculated from the histograms shown in Fig. 3

histograms and potential profiles are displayed in Figs. 3 and 4. The experimental potential profiles were linear least squares fitted with the superposition of a gravitational contribution and an electrostatic term. According to Prieve [15] this can be expressed as

$$\frac{\Delta\phi}{k_{\mathrm{B}}T} = \frac{G}{k_{\mathrm{B}}T}\left[\frac{1}{\kappa}(\exp\{-\kappa\Delta h\}-1)+\Delta h\right], \tag{8}$$

where $G = 4\pi R 3\Delta\rho g/3$ is the buoyancy corrected net weight of the sphere with $\Delta\rho$ the particles excess mass density and g the acceleration of gravity. According to Eq. 8 G can be directly extracted from the linear branch of the potential profiles at large Δh. The average value we get from the three potential profiles is $G \approx 0.08$ pN. The complete list of fitting parameters is given in Table 1. The full line in Fig. 4 was calculated using the mean values for G and κ^{-1} from Table 1, which shows that the experimental data for this case can be described by this simple model within an experimental error of about 10% for the gravitational part and of ca. 15% for the electrostatic repulsion.

However the situation changes dramatically when the probed coating consists of more than one polyelectrolyte layer. An example for the raw scattering data from a PSS sphere above a PEI/PSS double layer is shown in Fig. 5. The raw data are not anymore statistically distributed as in Fig. 2 but they rather appear to have two privileged mean values around which they fluctuate. Accordingly the histograms show two maxima. The experiments could not be reproduced, even if the same sphere is observed at different times. Furthermore we observe that contrary to the behavior of a PSA sphere above a single PEI-layer, the spheres do not move laterally, i.e. they stay in the area observed through the diaphragm for hours.When we applied a gentle flow with the peristaltic pump we usually use to exchange solvent in the sample cell, the probe particles were not displaced. They moved out of position for some particle diameters, but snapped back as soon as the pump was switched off. After 24 to 48 hours usually all particles are found to stick to the surface, which we did not observe for the single PEI-layer.

This behavior does not quantitatively change neither with the number of layers nor with the chemical nature of

Table 1 Net particle weight G and Debey screening length κ^{-1} obtained by fitting Eq. 8 to the potential profiles shown in Fig. 4. The values for the particle radii, R, were calculated from G assuming a constant excess mass density of $\Delta\rho = 0.05$ mg/mL

Sphere no.	G/pN	κ^{-1}/nm	R/μm
1	0.07	15	3.4
2	0.07	19	3.2
3	0.09	15	3.6

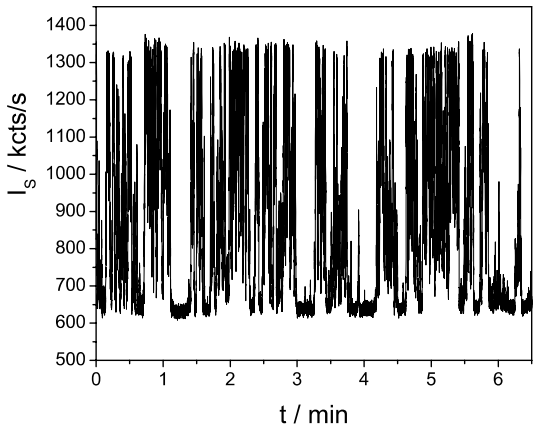

Fig. 5 Raw data of intensity vs time from a TIRM experiment on a 4.54 μm PSS sphere floating above a glass surface coated with a PEI/PSS double layer

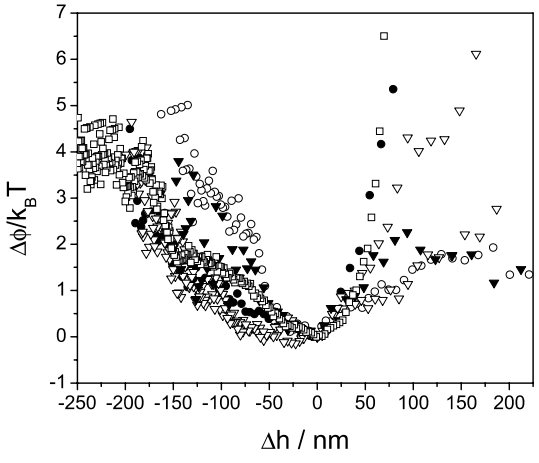

Fig. 6 Various interaction profiles of polystyrene latex spheres with PEM. *Circles*: 4.54 μm PSS spheres above eight PDADMAC/PSS double layers; *Down Triangles*: 4.54 μm PSS spheres above one PDADMAC/PSS double layer; *Square*: 2.92 μm PSA spheres above a PEI/PSS/PDADMAC assembly. *Open symbols* refer to a nominal Debye length of $\kappa^{-1} \approx 30$ nm, *full symbols* to $\kappa^{-1} \approx 14$ nm

the topmost layer nor with the strength of the electrostatic repulsion. This is demonstrated in Fig. 6 where we have collected randomly chosen potential profiles from various experiments under different conditions.

It is however noteworthy, that the width of the potential profiles extracted from these systems are much larger than observed for the PEI single layer. The repulsive part of the profiles generally extends over more than 200 nm. This is in agreement with the results of osmotic pressure measurements on PEM-coated silica particles reported recently [17]. These authors argue that the chains of the topmost polyelectrolyte layer at very low ionic strength may reach out into the surrounding solvent up to a distance of about half its contour length. Due to this chain stretching the electrostatic repulsion is caused to range much further than one would expect for a collapsed top layer based on DLVO calculations. Although we were working at moderate ionic strengths a similar effect might cause the long ranging repulsion also observed in our experiments.

While in the case of a PSA sphere above a single PEI layer the repulsive part of the potential can be attributed to gravity alone, this is not possible in all other cases. For this deviation we can offer only a speculative interpretation at the moment. It is in some cases possible to fit the experimental data to a harmonic potential profile, as if the probe sphere were stuck to a Hookian spring, which hints to the possibility that the particle might be adsorbed to a oppositely charged chain stretching out into the solvent. This requires that also the second layer from top is to a certain degree extended into the surrounding solution. Such a strong interdigitation between adjacent polyelectrolyte layers was detected in neutron reflectometry measurements [5, 7]. It was observed that polyanion layers may penetrate up to three consecutive polycation layers. If this holds also for the second layer from top, then chains from this layer can stretch out into the solution far enough to get in contact with the probe sphere. That might explain why the particles do not move laterally when floating above a multilayer and why the PSA sphere floating above single PEI layer behaves as expected. In this case there are no oppositely charged chains to which the probe sphere could stick.

In summary our experiments show that the interaction potential, which PEM deliver to their surroundings is not a simple laterally homogeneous DLVO-potential. Rather, the PEM is laterally inhomogeneous containing patches where electrostatic repulsion is over compensated by an attractive contribution to the interaction potential. The area fraction of these patches was roughly quantified with chemical probe experiments reported recently by Bosio et al. [14]. There the authors find that related PEM-systems cause adhesive forces to like charged spheres at about 30–50% of the locations probed. This behavior does, like in our experiments, not change with the number of layers. The reason for the existence of these adhesive areas is probably the strong interdigitation of adjacent polyelectrolyte layers.

Conclusions

We investigated the potential profiles between polyelectrolyte multilayers and spherical colloidal probes by total internal reflection microscopy. The interaction potential between a single PEI layer and a PSA sphere can be accurately described by the superposition of a pseudo-attractive part caused by gravity and a repulsive electrostatic contribution. If the polyelectrolyte assembly consists of more than one layer we observe that the experimental interaction profiles become irreproducible and that the probe spheres cease to move laterally. This is independent of the number

of layers and the charge sign of the top layer. As a common feature all profiles exhibit a repulsive part which is very long ranged. These findings are further support to earlier observations of PEM-layers being laterally inhomogeneous [14] and chains of the top layer stretching out into the surrounding solution [17].

References

1. Decher G (1997) Science 277:1232
2. Bertrand P, Jonas A, Laschewsky A, Legras R (2000) Macromol Rapid Commun 21:319 (and references therein)
3. Sukhorukov GB, Dontah E, Lichtenfeld H, Knippel E, Knippel M, Budde A, Möhwald H (1998) Colloids Surfaces A: Physicochem Eng Aspects 137:253
4. Farhat T, Yassin G, Dubas ST, Schlenoff JB (1999) Langmuir 15:6621
5. Schmitt J, Grünewald T, Decher G, Pershan PS, Kjaer K, Lösche M (1993) Macromolecules 26:7058
6. Tarabia M, Hong H, Davidov D, Kirstein S, Steitz R, Neumann R, Avny Y (1998) J Appl Phys 83:725
7. Lösche M, Schmitt J, Decher G, Bouwman WG, Kjaer K (1998) Macromolecules 31:8893
8. Steitz R, Jaeger W, v. Klitzing R (2001) Langmuir 17:4471
9. Glinel K, Moussa A, Jonas AM, Laschewsky A (2002) Langmuir 18:1408
10. Schoeler B, Kumaraswamy G, Caruso F (2002) Macromolecules 35:889
11. Voigt U, Jaeger W, Findenegg GH, v. Klitzing R (2003) J Phys Chem B 107:5273
12. Lowack K, Hem CA (1998) Macromolecules 31:823
13. Adamczyk Z, Zembala M, Warszynski P, Jachimska B (2004) Langmuir 20:10517
14. Bosio V, Dubreuil F, Bogdanovic G, Fery A (2004) Colloid And Surfaces A: Physicochem Eng Aspects 243:147
15. Prieve DC (1999) Adv Colloid Interface Sci 82:93
16. Prieve DC, Walz JY (1993) Appl Opt 32:1629
17. Schönhoff M (2005) Oral presentation L30A at the 42nd Meeting of the German Colloid Society, Aachen, Germany